Reduced-Order Modeling of Radiation Transport in Binary Stochastic Media

Aaron Olson,* Anil Prinja,[†] Brian Franke*

Radiation Effects Theory Department, Sandia National Laboratories, Albuquerque, NM
[†]*Department of Nuclear Engineering, University of New Mexico, Albuquerque, NM*
aolson@sandia.gov, prinja@unm.edu, bcfrank@sandia.gov

Abstract - *Binary stochastic media arise in several radiation transport applications including photon, neutron, or charged particle transport through clouds, plasma-air structures, heterogeneous radiation shields, and BWR coolant. Methods for solving transport quantities in such media have generally focused on simple material homogenization or closures for the stochastic transport equation, but yield accurate results only in special mixing regimes. In this work we demonstrate an efficient representation of binary stochastic media for radiation transport applications using a Nataf transformation coupled with a Karhunen-Loève expansion and further reduce the stochastic complexity using stochastic collocation. For some problems, this approach is more accurate than existing approximate methods while being less computationally expensive than brute force solution methods. Additionally, it can provide higher-order statistics of the solution response than currently used approximate methods, lends well to application in different mixing statistics, and provides a means by which to estimate and further resolve computational error.*

I. INTRODUCTION

Transport through binary stochastic media has been a topic of interest for a few decades [1, 2, 3, 4] and remains under active research [5, 6, 7, 8]. The grandest goal is to develop a method that is accurate, efficient, has quantifiable and reducible error, and can be applied to a wide range of material mixing types in one-, two-, or three-dimensional geometry. A close second to this goal is development of a suite of methods which each fill a niche and as a set achieve these attributes well enough for individual problems of interest.

Despite a growing suite of approaches to solving the transport equation involving stochastic media, the most widely used are the atomic mix (AM) approximation and the Levermore-Pomraning (LP) closure [1, 9, 10]. The atomic mix approximation homogenizes the material throughout the domain as if mixed at the atomic scale. It performs best in finely mixed, heavily scattering problems. It is the simplest of the methods to implement and can be utilized for any type of material mixing statistics, but is also generally the least accurate of the mainstream methods. The LP closure and its Monte Carlo equivalent [11] are exact for purely-absorbing media. It is generally more accurate than the AM approximation when scattering is extant, except in optically thick media where LP does not reproduce the correct atomic mix diffusion equation. The LP closure has been developed for application in materials with Markovian mixing statistics. Neither the AM approximation nor the LP closure provide estimates of the error of or second order information for quantities solved. Additionally the error yielded by these methods is not reducible without a modification of the method itself.

Another method often used to produce benchmark solutions for stochastic transport problems is to create a large ensemble of realizations of the random material and effect transport on each realization. It is accurate and provides a means for error estimation and reducibility, but is also very slow, relying on Monte Carlo convergence in stochastic space, and is limited to application in problems for which there exists a known method for creating realizations.

In this paper we examine a method for modeling binary stochastic media for transport computations by applying a Nataf transformation to the Karhunen-Loève (KL) expansion [12, 13]. This discontinuous Karhunen-Loève (DKL) method uses the autocovariance function of a random material to characterize the media in terms of a finite number of random variables. While we have only applied the method to materials with Markovian mixing, a topic of future work is to apply the method to materials with other covariance functions [13]. Characterization of stochastic media in terms of random variables using DKL enables the stochastic problem to be treated as a "classic" uncertainty quantification problem, and in addition to random sampling (RS) of the variables to create realizations, methods like stochastic collocation (SC) can be used to increase the efficiency of the approach. Since the KL expansion provides a naturally anisotropic set of random variables, we have used anisotropic SC, though other forms of efficient SC may be applied, such as sparse grids [14, 15, 16] and adaptive methods [16, 17]. We here demonstrate that the DKL method models stochastic media accurately within a second-order representation of the material mixing statistics, that it can be efficient when appropriate uncertainty quantification methods are applied, and that error can be reduced through additional computational cost. The method has been shown to provide means for estimating error [18] and to model materials with non-Markovian mixing statistics in multi-dimensional problems [12]. It is also possible to use other stochastic processes to model random media using principles of this approach [19].

Previous work by the authors using the KL expansion to model stochastic media [5, 18, 20, 21, 22] has primarily focused on modeling spatially continuous random media, whereas this paper builds on newer work [18] and uses the KL expansion to model spatially discontinuous random media for radiation transport applications.

II. STOCHASTIC TRANSPORT MODEL

The stochastic transport equation of interest is

$$\mu \frac{\partial \psi(x,\mu,\omega)}{\partial x} + \Sigma_t(x,\omega)\psi(x,\mu,\omega) =$$

$$\frac{\Sigma_s(x,\omega)}{2} \int_{-1}^{1} d\mu' \psi(x,\mu',\omega), \qquad (1)$$

$$0 \le x \le L; \qquad -1 \le \mu \le 1$$

$$\psi(0,\mu) = 2, \quad \mu > 0; \qquad \psi(L,\mu) = 0, \quad \mu < 0,$$

in which x and μ are the particle spatial and angular variables and the label ω denotes a material realization. We consider a Markovian mixture of two immiscible fluids in one-dimensional planar geometry, with chord lengths λ given by the exponential distribution [1, 10]:

$$p(\lambda) = \frac{1}{\Lambda_i} \exp\left[-\frac{\lambda}{\Lambda_i}\right], \qquad (2)$$

where Λ_i is the average chord length in material i, $i = \{0, 1\}$. Two realizations of the mixture, obtained by successively sampling the chord length distribution in each material, are shown in Fig. 1. The likelihood of Material 0 at a randomly chosen location x in a realization ω of the material is computed as

$$p_0 = \frac{\Lambda_0}{\Lambda_0 + \Lambda_1}, \qquad (3)$$

and the correlation length of the material is solved as

$$\lambda_c = \frac{\Lambda_0 \Lambda_1}{\Lambda_0 + \Lambda_1}. \qquad (4)$$
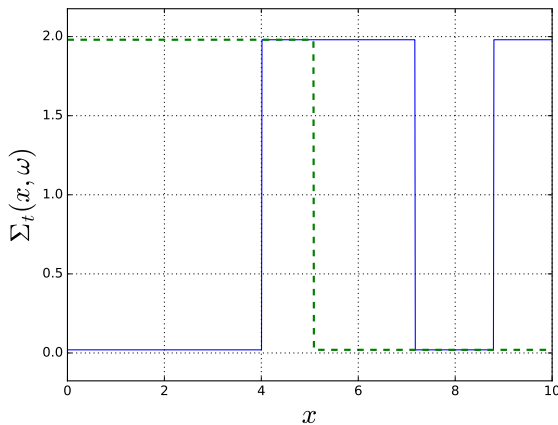
Fig. 1. Example benchmark realizations

In this work, we use a nonlinear transformation and the Karhunen-Loève theorem to map the discontinuous random field representing the material mixing to a finite number of Gaussian-distributed random variables that allows application of stochastic collocation techniques [16] to transport in binary

mixtures. The stochasticity of the media is represented by random material index Z, such that either Material 0 or Material 1 exists at each point x in each realization ω:

$$Z(x,\omega) = \begin{cases} 0 & \text{if in Material 0} \\ 1 & \text{if in Material 1} \end{cases} \qquad (5)$$

The autocovariance of process Z for media with Markovian mixing is exponential:

$$C_Z(x,x') = \sigma^2 \exp\left[-\frac{|x-x'|}{\lambda_c}\right], \qquad (6)$$

where σ^2 is the variance of process Z. Scattering and total macroscopic cross sections $\Sigma_u(x,\omega), u = \{s, t\}$ are represented in terms of this discontinuous random process:

$$\Sigma_u(x,\omega) = \Sigma_{u,Z(x,\omega)}. \qquad (7)$$

1. Nataf Transformation

The Nataf transformation [12, 13, 19] is used to map the random medium to a Gaussian random process g with a covariance that is related nonlinearly to the original covariance by equating marginal distributions for the original and Gaussian fields and solving for the value of $g(x,\omega)$ corresponding to the probability of Material 0:

$$\int_{-\infty}^{g^*} \frac{1}{2\pi} \exp\left[-\frac{\xi^2}{x}\right] d\xi = p_0 \qquad (8a)$$

$$\Rightarrow g^* = \sqrt{2}\, \text{erf}^{-1}(2p_0 - 1). \qquad (8b)$$

The mean and variance of process Z are shown to be:

$$\mu = 1 - p_0 \qquad (9a)$$

$$\sigma^2 = p_0(1 - p_0) \qquad (9b)$$

The random material index written more explicitly is

$$Z(x,\omega) = c\,(g(x,\omega)) = \begin{cases} 0 & \text{if } g(x,\omega) \le g^* \\ 1 & \text{if } g(x,\omega) > g^*, \end{cases} \qquad (10)$$

where $c(g)$ is shorthand for the function mapping $g(x,\omega)$ to $Z(x,\omega)$. The relationship between the covariance functions of the original random medium and the Gaussian field follows from the mapping and two-point averaging:

$$C_Z(x,x') = \frac{\mathbb{E}\left[(Z(x) - \mu)(Z(x') - \mu)\right]}{\sigma^2}$$

$$= \int_{-\infty}^{\infty} \int_{-\infty}^{\infty} \frac{(c(x) - \mu)(c(x') - \mu)}{\sigma^2} p_g(x, x', C_g(r)) dx dx', \qquad (11a)$$

where r represents the absolute distance between x and x', $r = |x - x'|$, and p_g is the standard bivariate Gaussian distribution,

$$p_g(x, x', C_g(r)) = \frac{1}{2\pi \sqrt{1 - C_g^2(r)}} \exp\left(-\frac{x^2 + x'^2 - 2C_g(r)xx'}{2(1 - C_g^2(r))}\right). \qquad (11b)$$

2. Numerical Solution of Gaussian Process Covariance

Equation (11) relates the known covariance of the discontinuous process C_Z to the yet unknown covariance of the Gaussian field C_g, but C_g must still be solved from this transcendental relationship. In previous work, including in Ref. [18], we solved values of C_g using a method very similar to that in Refs. [12, 13], in which the bivariate Gaussian is expanded in terms of Hermite polynomials and reduced to an expansion of single integrals. In this work we choose to solve C_g through direct numerical evaluation of the double integral in Eq. (11) as described below and as performed in Ref. [19]. We have investigated a third method in which we perform a change of variables to map to integrals from zero to infinity, multiply Eq. (11a) by $e^{y-y'+y'-y'}$ where y and y' are the new integration variables, absorb the e^y and $e^{y'}$ terms in the Eq. (11) exponential, and use the remaining e^{-y} and $e^{-y'}$ terms to form the basis for global Gauss-Laguerre integration.

Whereas all three methods for solving C_g were effective for values of C_Z (and thus C_g) much less than 1.0, all three methods break down due to numerical issues as covariance values approach 1.0. Ref. [12] made note of this phenomenon by saying that "there were numerical problems when $R_{ZZ} \approx 1$". Using SciPy integrators ("integrate.quad()" in the Hermite expansion case and "integrate.nquad()" in the direct integration case) and SciPy-generated Gauss-Laguerre nodes and weights [23], we found the Hermite-expansion-based method to be the most limited due to numerical difficulties near 1.0, the Gauss-Laguerre method to be the second most limited, and the direct integration method to be the least limited. We acknowledge, as observed in Ref. [13], that the Hermite expansion method is more computationally efficient than direct integration; perhaps a smart approach which prefers the Hermite expansion method but switches to the direct integration method when covariance values approach 1.0 would be most appropriate. Additionally, we hypothesize that if using a higher quadrature order than the 100 points provided by current SciPy packages, the Gauss-Laguerre method may be able to solve covariance values closer to 1.0, and may be able to do it more efficiently, than the direct integration method. Nonetheless in this work we have used the direct integration method described below since we found it to resolve covariance values closer to 1.0 than the other methods.

We begin numerical integration of Eq. (11) by recognizing that the term $(Z(x) - \mu)(Z(x') - \mu)/\sigma^2$ is equal to one of three values based on the domain of integration:

$$\frac{(Z(x) - \mu)(Z(x') - \mu)}{\sigma^2} =$$

$$\begin{cases} \frac{1-p_0}{p_0} & \text{if } x \in (-\infty, g^*], x' \in (-\infty, g^*] \\ -1 & \text{if } x \in (-\infty, g^*], x' \in (g^*, \infty) \\ -1 & \text{if } x \in (g^*, \infty), x' \in (-\infty, g^*] \\ \frac{p_0}{1-p_0} & \text{if } x \in (g^*, \infty), x' \in (g^*, -\infty) \end{cases} \quad (12)$$

Substituting Eq. (12) into Eq. (11a) and reorganizing yields

$$C_Z(r) = - \quad 1 \quad \int_{-\infty}^{\infty} \int_{-\infty}^{\infty} p_g(x, x', C_g(r)) dx dx'$$
$$+ \frac{1}{p_0} \int_{-\infty}^{g^*} \int_{-\infty}^{g^*} p_g(x, x', C_g(r)) dx dx' \quad (13)$$
$$+ \frac{1}{1-p_0} \int_{g^*}^{\infty} \int_{g^*}^{\infty} p_g(x, x', C_g(r)) dx dx'.$$

Recognizing that p_g is normalized to 1 when integrated over the whole domain, Eq. (13) further reduces to

$$C_Z(r) = -1 + \frac{1}{p_0} \int_{-\infty}^{g^*} \int_{-\infty}^{g^*} p_g(x, x', C_g(r)) dx dx'$$
$$+ \frac{1}{1-p_0} \int_{g^*}^{\infty} \int_{g^*}^{\infty} p_g(x, x', C_g(r)) dx dx'. \quad (14)$$

At values of r, a root-finding algorithm may be used over $C_g(r)$ to find the value which minimizes the residual τ in

$$\tau = \Big| - C_Z(r) + \Big(- 1$$
$$+ \frac{1}{p_0} \int_{-\infty}^{g^*} \int_{-\infty}^{g^*} p_g(x, x', C_g(r)) dx dx' \quad (15)$$
$$+ \frac{1}{1-p_0} \int_{g^*}^{\infty} \int_{g^*}^{\infty} p_g(x, x', C_g(r)) dx dx' \Big) \Big|;$$

we use SciPy's "optimize.brentq()" root finder and integrate using SciPy's "integrate.nquad()" routine to solve for $C_g(r)$ at uniformly spaced values of r.

While we have found this approach to directly solve values of $C_g(r)$ considerably closer to 1.0 than the other methods, the algorithm still fails to solve values very close to 1.0. In Ref. [12] these values were "interpolated linearly in those situations". We test this approach, and that of using global polynomial fits based on the $C_g(r = 0) = 1$ point and all values of $C_g(r)$ which have been successfully solved, accepting the interpolation which minimizes the L_2 norm comparing the original values of C_Z and those yielded by a forward solve of Eq. (11). This approach is described in more detail in Ref. [18]. Highly correlated media, such as in some cases examined later in this paper, do not yield to direct solution of $C_g(r)$ for any values of r which exist in the domain of the problem, vis., for $r \in [0, L]$. In these cases, we continue attempting to solve for larger values of r until interpolation can be made. This approach enable solution of $C_g(r)$ for all problems examined in Refs. [9, 10].

3. Karhunen-Loève Expansion

Once the covariance of the Gaussian field has been computed, realizations of the field are generated using a Karhunen-Loève (KL) representation [16], the optimal, mean-squared, and error-minimizing expansion of a second-order random process:

$$g(x, \omega) = \sum_{k=0}^{\infty} \sqrt{\gamma_k} u_k(x) \xi_k(\omega), \quad (16)$$

where γ_k, $u_k(x)$, and $\xi_k(\omega)$ are the eigenvalue, eigenfunction, and random variable of the k-th term of the KL expansion

in which terms are ordered such that eigenvalues γ_k decrease monotonically. Eigenfunctions $u_k(x)$ here characterize variation over one-dimensional physical space ($x \in [0, L]$). In practice, the KL expansion must be truncated at some finite order K, such that random variables $\xi_k(\omega)$ characterize variation over K-dimensional stochastic space ($\xi_k \in \mathcal{N}(0, 1) \forall k, k \in \{1, \ldots, K\}$). Eigenvalue decay is more rapid for more highly correlated systems such that less terms K are required to accurately represent the process. The KL expansion is therefore more efficient for more highly correlated systems. Eigenvalues and eigenfunctions (or eigenvectors) are obtained from solution of the Fredholm equation:

$$\int_0^L C_g(x, x')u(x')dx' = \gamma u(x), \tag{17}$$

where $C_g(x, x')$ is the two-point autocovariance of the KL process. The random variables are independent since we map to Gaussian random variables, KL random variables are uncorrelated, and uncorrelated Gaussian random variables are independent.

4. Numerical Solution of Eigenvalues and Eigenvectors

Eigenvalues and eigenfunctions must be solved using the numerical covariance function $C_g(x, x')$ as the kernel for the Fredholm equation (Eq. (17)). We solve using the Nyström method [24, 25] and choose a uniform discretization scheme of order N_{Ny} such that covariance values solved in the Nataf transformation align with nodes of the Nyström discretization:

$$\sum_{j=1}^{N_{Ny}} w_j C_g(x_i, x_j)u_k(x_j) = \gamma_k u_k(x_i), \quad k = 1, \ldots, N_{Ny}. \tag{18}$$

This equation is written in matrix notation as

$$\mathbf{CW}\mathbf{u}_k = \gamma_k \mathbf{u}_k, \tag{19}$$

where matrix $\mathbf{C}$ is a symmetric positive semi-definite matrix with elements $C_{ij} = C_g(x_i, x_j)$, matrix $\mathbf{W}$ is a diagonal matrix with values w_j, and vector $\mathbf{u}_k$ spans the physical domain for each eigenvalue k. Eq. (19) is re-written as

$$\mathbf{B}\mathbf{u}_k^* = \gamma_k \mathbf{u}_k^*, \tag{20a}$$

$$\mathbf{B} = \mathbf{W}^{\frac{1}{2}}\mathbf{CW}^{\frac{1}{2}}; \quad \mathbf{u}_k^* = \mathbf{W}^{\frac{1}{2}}\mathbf{u}_k, \tag{20b}$$

where $\mathbf{W}^{-\frac{1}{2}}$ is the diagonal matrix with values $\sqrt{w_j}$. The eigenvector is then solved as

$$\mathbf{u}_k = \mathbf{W}^{-\frac{1}{2}}\mathbf{u}_k^*. \tag{21}$$

We linearly interpolate between nodes of $\mathbf{u}_k$ when x exists between Nyström nodes, $x \in (x_1, x_{N_{Ny}})$, and otherwise defer to a more expensive mapping method given in the Nyström theory:

$$u_k(x) = \frac{1}{\gamma_k} \sum_{j=1}^{N_{Ny}} \sqrt{w_j}\mathbf{u}_{k,j}^* C_g(x, x_j). \tag{22}$$

Assuming uniform sampling of the KL expansion throughout the domain, the expectation of the cost of one discontinuous Karhunen-Loève (DKL) evaluation is roughly equal to $CK\left[1 + 2\frac{N_{Ny}-1}{N_{Ny}}\right]$, where K is the number of KL terms kept in truncation and C is the cost of sampling from an eigenvector. By precomputing values of $u_k(x = 0)$ and $u_k(x = L)$ using Eq. (22) and linearly interpolating throughout the whole domain thereafter the cost can be reduced to $2CK$. A further reduction in cost could be achieved by solving values of $g(x, \omega)$ at each of the N_{Ny} nodal locations in x for each realization ω; the cost of subsequent sampling of DKL would then be roughly $2C$.

5. Material Modeling Results

Figures 2 and 3 show the exponential material index covariance function C_Z, the computed covariance of the Gaussian process C_g, and the material process covariance observed C_Z^* by sampling 10^5 times for each plotted value of r from 10^5 realizations for each of two cases described in Section IV. In the L=10.0 case, 4 of the 250 values of $C_g(r)$ were not solved directly but were interpolated, and in the L=1.0 case, 39 of the 250 values were interpolated. Figure 4 shows two realizations generated using the Nataf transformation with the same input parameters as Fig. 1. Figure 5 shows the input and observed process mean and standard deviation in which observed values were computed at each location x by sampling from 10^6 realizations. These plots were generated using a KL truncation of $K = 5$ and the input parameters for Case 3a (defined in Section IV.) with either L=1.0 or L=10.0. The observed covariance function, mean, and standard deviation converge towards the input values with larger values of K and more random samples.

III. STOCHASTIC SOLUTION METHODS

While the truncated Karhunen-Loève expansion characterizes the stochastic variability in terms of a finite number of random variables, a solution method method must still be used to resolve the effects of stochastic variation. The expectation of moment m of transport result φ is solved as

$$\mathbb{E}\left[\varphi^m\right] = \int_{\xi_N} d\xi_N \cdots \int_{\xi_1} d\xi_1 \; \varphi^m(x, \boldsymbol{\xi}) \prod_{n=1}^{N} p(\xi_n), \tag{23}$$

where $\boldsymbol{\xi}$ is a multi-index of ξ_n values ($\boldsymbol{\xi} := \{\xi_1, \ldots, \xi_N\}$) and $p(\xi_n)$ is the probability density for ξ_n.

We solve the integral in Eq. (23) in one of two ways. The first is random sampling (RS), often called Monte Carlo sampling, in stochastic space:

$$\mathbb{E}\left[\varphi^m\right] \approx \frac{1}{R} \sum_{i=1}^{R} \varphi^m(x, \xi_1^{(i)}, \ldots, \xi_K^{(i)}), \tag{24}$$

where R is the number of samples and $\xi_k^{(i)}$ is the randomly chosen node of the i-th sample. The error of the expectation of moments converges as $R^{-\frac{1}{2}}$ regardless of the number of stochastic dimensions.
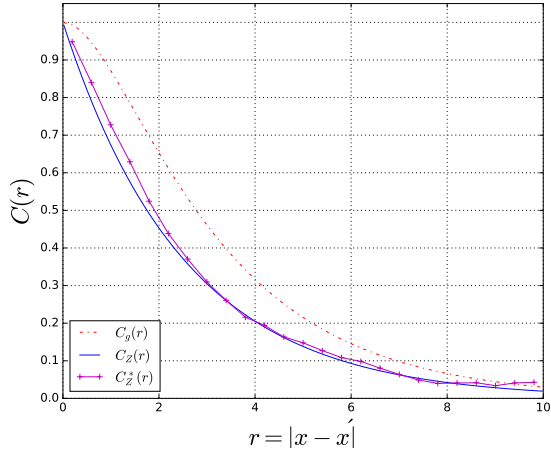
Fig. 2. Input and observed covariance functions, L=10.0
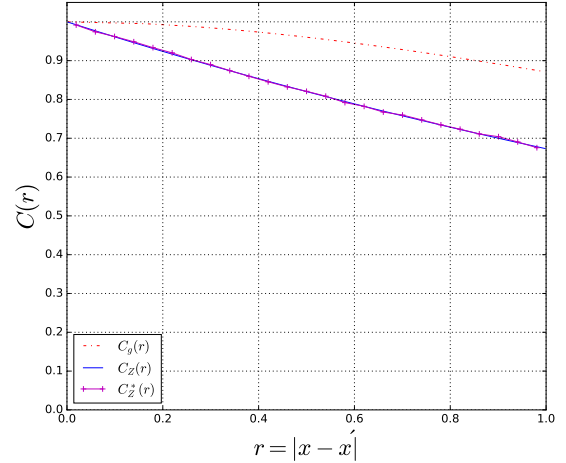
Fig. 3. Input and observed covariance functions, L=1.0
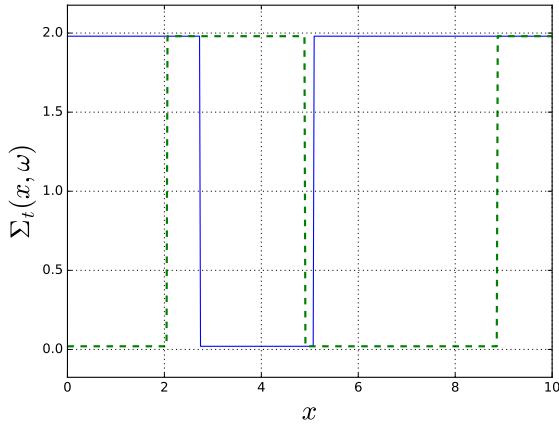
Fig. 4. Example DKL-generated realizations, L=10.0
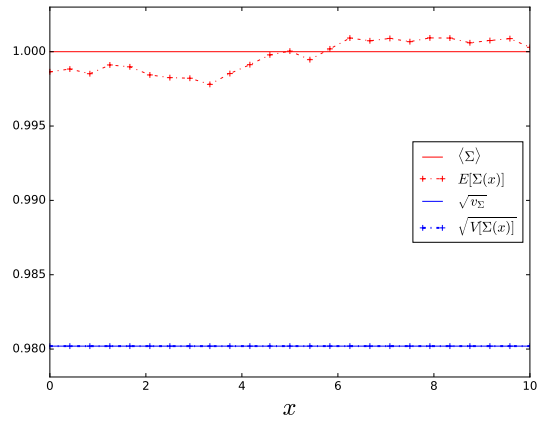
Fig. 5. Input and observed mean and deviation, L=10.0

We secondly solve Eq. (23) using a form of deterministic sampling, stochastic collocation (SC):

$$\mathbb{E}\left[\varphi^m\right] \approx \sum_{q_K}^{Q_K} \cdots \sum_{q_1}^{Q_1} w_1^{(q_1)} \cdots w_K^{(q_K)} \varphi^m(x, \xi_1^{(q_1)}, \ldots, \xi_K^{(q_K)}),$$

(25)

in which $w_k^{(q_k)}$, $\xi_k^{(q_k)}$, and Q_k are collocation weights, nodes, and quadrature orders for dimension k. The error of the expectation of moments converges exponentially for sufficiently smooth response surfaces, though the convergence rate diminishes with a lack of regularity and with larger numbers of stochastic dimensions. If the KL expansion is truncated to few enough dimensions K and the response is sufficiently smooth, SC is considerably more efficient than RS, especially with well-chosen quadrature orders $\boldsymbol{Q} := \{Q_1, \ldots, Q_K\}$.

IV. NUMERICAL RESULTS

The transport results in this paper compare the performance of the discontinuous Karhunen-Loève (DKL) method to that of the benchmark method of brute force computation

from randomly sampled realizations, the atomix mix (AM) approximation, and the Levermore-Pomraning (LP) closure for 24 of the 27 cases that have become a classic set for transport in binary stochastic media with Markovian mixing [9, 10]. Transmittance and reflectance values are first compared for all 24 cases using relatively cheap DKL parameters to demonstrate the applicability of the method to the problem set. More converged and expensive parameters are then used for two cases to demonstrate the ability to further resolve error. Internal flux profiles and leakage probability density functions (pdfs) are then compared to those given by the other methods to further demonstrate the accuracy of the method.

The cases solved in this paper are designated in terms of a case number, a case letter, and a slab thickness. In the literature they are typically defined by average material chord lengths Λ_i, total cross section values $\Sigma_{t,i}$, and scattering ratios $c_i = \Sigma_{s,i}/\Sigma_{t,i}$, though we utilize the probability of Material 0 p_0 and the correlation length λ_c (note Eqs. (3) and (4)) instead of the average material chord lengths to uniquely describe the cases. The cases are defined in Table I. We solve 24 of the 27 cases, omitting the three which have the weakest correlation

TABLE I. Benchmark Set Parameters

Case Num.	$\Sigma_{t,0}$	$\Sigma_{t,1}$	p_0	λ_c
1	10/99	100/11	0.9	0.099
2	10/99	99/10	0.9	0.99
3	2/101	200/101	0.5	2.525

Case Let.	c_0	c_1	Slab Thickness	
a	0.0	1.0	$L =$	0.1
b	1.0	0.0	$L =$	1.0
c	0.9	0.9	$L =$	10.0

relative to the size of the material slab and thus require many KL terms for accurate representation.

Benchmark results are computed by effecting transport with analog Monte Carlo using $N = 10^5$ particle histories on each of $R = 10^5$ realizations generated by sampling successive material chord lengths using Eq. (2). Atomic mix and Levermore-Pomraning results are generated using $N = 10^7$ particle histories. For results generated with the new discontinuous KL method, transport is effected on each realization using Woodcock Monte Carlo [26] with $N = 10^5$ particle histories. When using stochastic collocation an anisotropic set of quadrature orders, $\mathbf{Q} = \{5, 4, 4, 3, 3\}$, is chosen yielding $R = 720$ realizations whereas $R = 10^5$ realizations are employed for random sampling. In all stochastic collocation cases and two of the four random sampling cases $K = 5$ KL terms are kept in truncation; in the remaining two random sampling cases $K = 15$. In all cases a Nataf and Nyström grid of size $N_{Ny} = 250$ has been chosen.

Woodcock Monte Carlo is utilized so that material boundary locations need not be solved to effect transport. This is not a difficult task for our one-dimensional problems, but not needing to explicitly solve material boundary locations is expected to be a useful attribute in multi-dimensional problems.

The values of K, N_{Ny}, N, $\mathbf{Q}$, and R used to compute the results in this paper are likely not the optimal choices, but have been selected to show a cross section of results. For many cases it would be preferable to choose parameters which converge the solution more and are best chosen from the results of a convergence study [18] or the results of an adaptive algorithm such as that presented in Ref. [17].

We estimate the error in the mean leakage values due to Monte Carlo transport and either random sampling or stochastic collocation in the benchmark solutions and DKL solutions to range from about 0.6% for small mean values, e.g., 0.0005, to about 0.03% for large mean values, e.g., 0.95. Similarly, we estimate the Monte Carlo error in AM and LP mean leakage values to range from about 0.03% to about 0.002%.

Tables II and III contain transmittance and reflectance means ($\langle T \rangle$ and $\langle R \rangle$), standard deviations (σ_T and σ_R), and their errors relative to the computed benchmark solutions (ε_{rel}) for each of the 24 cases. Relative errors are computed for quantity-of-interest φ as

$$\varepsilon_{rel} = \frac{\varphi_{Bench.} - \varphi_{approx.}}{\varphi_{Bench.}}. \qquad (26)$$

With the relatively crude parameters chosen to make the DKL computations, the method produces mean values that are more accurate than AM in nearly all cases and that are more accurate

than LP in some cases while being much cheaper than the benchmark method. We also note that the DKL method is the only method other than the benchmark which provides second-order information for quantities-of-interest, and that the error in these quantities is not excessive.

We examine the effectiveness of stochastic collocation and demonstrate the ability to reduce the error with an increased number of KL terms for two cases: Case 2a, L=10.0, in which the error in the initial results are relatively high, and Case 3a, L=10.0, in which the error in the initial results is already less than that given by LP. These cases are solved a second time using random sampling ($R = 10^5$) instead of stochastic collocation ($R = 720$) with the same number of KL terms, $K = 5$. For the four mean values yielded and three of the four standard deviation values the error was greater for the large RS ensemble than when using the cheap instantiation of stochastic collocation; this demonstrates how effective anisotropic SC can be. These cases are further solved using RS by increasing the number of KL terms to $K = 15$, and for all results the yielded error is much less than that given by the other approximate solution methods; this demonstrates the ability to reduce the error yielded by the method through additional computational cost. Reduction of error through keeping more KL terms is applicable to each case such that the error yielded can be reduced to less than that given by the approximate methods. Error can be reduced by increasing K, N, R or $\mathbf{Q}$, and N_{Ny}, though we do not believe the error due to the value of N_{Ny} to be significant compared to the other error sources for these problems and parameter sets. The only truly irreducible error in the DKL method is the bias introduced in the KL limitation of describing only second-order statistics, while other numerical error sources include the accuracy of the solution method used for acquiring the Gaussian process covariance and the limitations of machine precision.

Transport results are further examined for Cases 2a and 3a with L=10.0 in Figures 6 through 13. Flux mean and relative standard deviation values, computed by tallying in 100 evenly spaced cells, and leakage pdfs are plotted.

For Case 3a, L=10.0 the DKL mean flux values are much better than AM and LP values with $K = 5$, and nearly indistinguishable to the eye from benchmark values when using $K = 15$. Flux relative standard deviation values show the crudeness of the SC parameters chosen, though the values are still close to the benchmark values, solutions are improved using RS, and solutions are further improved by keeping more KL terms. The $K = 5$ versions of both cases capture the behaviors of the leakage pdfs and the $K = 15$ results show convergence towards the benchmark distributions.

As expected from the accuracy of the leakage results, Case 2a, L=10.0 results show similar behaviors as the Case 3a results, but are less accurate. The $K = 5$ version of the mean flux profile almost exactly matches the LP profile and the $K = 15$ mean flux profile is more accurate, nearly matching the benchmark results. The $K = 5$ RS and SC relative standard deviation flux values show a similar level of accuracy as one another though the RS results fluctuate less. The $K = 15$ results show an improvement in accuracy. Leakage pdfs again show considerable agreement and convergence towards the benchmark solution as more KL terms are kept.

TABLE II. Transmittance Values and Errors

Case Desig.		L	Transmittance Mean, $\langle T \rangle$				Relative Error, ε_{rel}			σ_T		ε_{rel}
			Bench.	AM	LP	DKL	AM	LP	DKL	Bench.	DKL	DKL
Selected Cases Solved with $K=5$, $\mathbf{Q}=\{5,5,4,4,3\}$, $N=100,000$												
1	a	0.1	0.93375	0.90689	0.93465	0.91543	0.029	-0.001	0.020	0.11203	0.11898	-0.062
		1.0	0.59598	0.48104	0.62734	0.65981	0.193	-0.053	-0.107	0.21517	0.21929	-0.019
	b	0.1	0.90131	0.83908	0.90086	0.86407	0.069	0.000	0.041	0.21070	0.23009	-0.092
		1.0	0.48524	0.23081	0.48433	0.60463	0.524	0.002	-0.246	0.36411	0.38736	-0.064
	c	0.1	0.93401	0.90603	0.93477	0.91277	0.030	-0.001	0.023	0.13345	0.14027	-0.051
		1.0	0.60089	0.47485	0.62739	0.68055	0.210	-0.044	-0.133	0.28402	0.28915	-0.018
2	a	0.1	0.93946	0.90689	0.93932	0.88863	0.035	0.000	0.054	0.12002	0.16664	-0.388
		1.0	0.72655	0.48104	0.74069	0.68196	0.338	-0.019	0.061	0.23000	0.26736	-0.162
		10.0	0.09848	0.00476	0.12834	0.14020	0.952	-0.303	-0.424	0.08921	0.09420	-0.056
	b	0.1	0.91481	0.83908	0.91422	0.82104	0.083	0.001	0.102	0.22067	0.30706	-0.392
		1.0	0.75941	0.23081	0.75904	0.69841	0.696	0.000	0.080	0.33317	0.38590	-0.158
		10.0	0.19601	0.00001	0.17934	0.33084	1.000	0.085	-0.688	0.25552	0.27005	-0.057
	c	0.1	0.94010	0.90603	0.93988	0.87903	0.036	0.000	0.065	0.14414	0.20014	-0.389
		1.0	0.76843	0.47485	0.77421	0.70647	0.382	-0.008	0.081	0.30066	0.35607	-0.184
		10.0	0.18715	0.00387	0.19478	0.28515	0.979	-0.041	-0.524	0.21406	0.22900	-0.070
3	a	0.1	0.92296	0.91478	0.92319	0.91905	0.009	-0.000	0.004	0.07237	0.05101	0.295
		1.0	0.65994	0.54455	0.66598	0.60953	0.175	-0.009	0.076	0.26829	0.20621	0.231
		10.0	0.16340	0.06681	0.24032	0.17415	0.591	-0.471	-0.066	0.17597	0.19461	-0.106
	b	0.1	0.85155	0.83335	0.85181	0.84294	0.021	-0.000	0.010	0.14499	0.10232	0.294
		1.0	0.48187	0.22070	0.48306	0.36466	0.542	-0.002	0.243	0.43605	0.34816	0.202
		10.0	0.07639	0.00001	0.07565	0.09643	1.000	0.010	-0.262	0.22537	0.25820	-0.146
	c	0.1	0.91440	0.90603	0.91468	0.91045	0.009	-0.000	0.004	0.08261	0.05819	0.296
		1.0	0.60415	0.47485	0.60919	0.54671	0.214	-0.008	0.095	0.33426	0.25515	0.237
		10.0	0.10412	0.00387	0.11971	0.11644	0.963	-0.150	-0.118	0.23034	0.25723	-0.117
Selected Cases Solved with $K=5$, $R=100,000$, $N=100,000$												
2	a	10.0	0.09848	0.00476	0.12834	0.14351	0.952	-0.303	-0.457	0.08921	0.09354	-0.049
3	a	10.0	0.16340	0.06681	0.24032	0.17643	0.591	-0.471	-0.080	0.17597	0.19644	-0.116
Selected Cases Solved with $K=15$, $R=100,000$, $N=100,000$												
2	a	10.0	0.09848	0.00476	0.12834	0.09812	0.952	-0.303	0.004	0.08921	0.09160	-0.027
3	a	10.0	0.16340	0.06681	0.24032	0.16456	0.591	-0.471	-0.007	0.17597	0.17845	-0.014

The widths of some pdf features, such as the right-most peak in Fig. 13, are largely an artifact of the number of particle histories used–a computation using only $N = 10^4$ particle histories not shown in this paper yielded a much wider peak. This peak corresponds to realizations containing only the more optically thin material and the true peak for this problem is a delta function with a probability equal to the likelihood of sampling a realization of only that material.

V. CONCLUSIONS

We described use of the Nataf transformation coupled with the Karhunen-Loève expansion to represent and reconstruct binary random mixtures in 1D planar geometry, including brief discussion of two methods and a detailed description of a third method used here for solving the necessary Gaussian process covariance in the Nataf transformation. We compared the performance of the new method solved using Woodcock sampling with benchmark, atomic mix, and Levermore-Pomraning transport results on a popular suite of benchmark problems demonstrating the accuracy of the method on the problem suite. For a cheap set of solution parameters using anisotropic stochastic collocation, the new method performed respectably compared to other approximate methods. The new method was shown to be more accurate than other approximate methods when using costlier problem parameters, demonstrating the reducibility of solution error with increased computational cost. Problem-dependent convergence studies could be used to choose the most appropriate solution parameters which would, in many cases, produce solutions more accurate than approximate methods while being more efficient than benchmark solutions. Convergence studies could also be used to produce error estimates, a trait particularly useful in problems with no known method for generating benchmark solutions. The method is believed to be applicable to materials which obey statistical mixing that is not Markovian, including material mixing types for which there is no known benchmark, and to be applicable in multi-dimensional problems. Investiga-

TABLE III. Reflectance Values and Errors

Case Desig.		L	Reflectance Mean, $\langle R \rangle$				Relative Error, ε_{rel}			σ_R		ε_{rel}
			Bench.	AM	LP	DKL	AM	LP	DKL	Bench.	DKL	DKL
Selected Cases Solved with K=5, $\mathbf{Q}$={5,5,4,4,3}, N=100,000												
1	a	0.1	0.04854	0.07524	0.04761	0.06744	-0.550	0.019	-0.389	0.11697	0.12367	-0.057
		1.0	0.25070	0.36009	0.21879	0.18304	-0.436	0.127	0.270	0.23574	0.23803	-0.010
	b	0.1	0.00859	0.00651	0.00847	0.00809	0.242	0.013	0.057	0.00294	0.00325	-0.108
		1.0	0.05416	0.01878	0.04556	0.06560	0.653	0.159	-0.211	0.03011	0.02866	0.048
	c	0.1	0.04794	0.07436	0.04699	0.06397	-0.551	0.020	-0.335	0.09303	0.10073	-0.083
		1.0	0.25411	0.35255	0.21683	0.20553	-0.387	0.147	0.191	0.15495	0.16371	-0.056
2	a	0.1	0.04284	0.07524	0.04298	0.09608	-0.756	-0.003	-1.243	0.12578	0.17457	-0.388
		1.0	0.12105	0.36009	0.10694	0.17014	-1.975	0.117	-0.405	0.27074	0.30723	-0.135
		10.0	0.23651	0.49523	0.18048	0.14728	-1.094	0.237	0.377	0.28587	0.25918	0.093
	b	0.1	0.00882	0.00651	0.00879	0.00758	0.262	0.004	0.141	0.00295	0.00407	-0.378
		1.0	0.07329	0.01878	0.07056	0.06960	0.744	0.037	0.050	0.02734	0.02948	-0.078
		10.0	0.28779	0.01962	0.21827	0.35822	0.932	0.242	-0.245	0.16317	0.14308	0.123
	c	0.1	0.04227	0.07436	0.04234	0.08382	-0.759	-0.002	-0.983	0.09800	0.13620	-0.390
		1.0	0.14246	0.35255	0.12422	0.16986	-1.475	0.128	-0.192	0.14494	0.16915	-0.167
		10.0	0.43290	0.47776	0.28961	0.40359	-0.104	0.331	0.068	0.05730	0.06081	-0.061
3	a	0.1	0.07507	0.08325	0.07483	0.07896	-0.109	0.003	-0.052	0.07432	0.05240	0.295
		1.0	0.32121	0.43589	0.31515	0.37137	-0.357	0.019	-0.156	0.28578	0.21864	0.235
		10.0	0.69161	0.78600	0.60778	0.67835	-0.136	0.121	0.019	0.26252	0.28233	-0.075
	b	0.1	0.00098	0.00070	0.00099	0.00086	0.289	-0.008	0.118	0.00098	0.00071	0.275
		1.0	0.00872	0.00195	0.00837	0.00707	0.776	0.040	0.189	0.00903	0.00767	0.150
		10.0	0.03633	0.00203	0.02400	0.04284	0.944	0.339	-0.179	0.04946	0.05361	-0.084
	c	0.1	0.06622	0.07436	0.06602	0.07013	-0.123	0.003	-0.059	0.06380	0.04502	0.294
		1.0	0.24320	0.35255	0.23730	0.29217	-0.450	0.024	-0.201	0.19844	0.15663	0.211
		10.0	0.44514	0.47776	0.32618	0.43751	-0.073	0.267	0.017	0.09300	0.10584	-0.138
Selected Cases Solved with K=5, R=100,000, N=100,000												
2	a	10.0	0.23651	0.49523	0.18048	0.14222	-1.094	0.237	0.399	0.28587	0.25628	0.103
3	a	10.0	0.69161	0.78600	0.60778	0.67683	-0.136	0.121	0.021	0.26252	0.28453	-0.084
Selected Cases Solved with K=15, R=100,000, N=100,000												
2	a	10.0	0.23651	0.49523	0.18048	0.23445	-1.094	0.237	0.009	0.28587	0.28479	0.004
3	a	10.0	0.69161	0.78600	0.60778	0.68896	-0.136	0.121	0.004	0.26252	0.26417	-0.006

tion and demonstration of these properties are topics of future work.

VI. ACKNOWLEDGMENTS

REFERENCES

1. G. C. POMRANING, *Linear kinetic theory and particle transport in stochastic mixtures*, World Scientific Publishing Co. Pte. Ltd., River Edge, New Jersey USA, 1st ed. (1991).

2. T. J. DONOVAN and Y. DANON, "Application of Monte Carlo chord-length sampling algorithms to transport through a two-dimensional binary stochastic mixture," *Nuclear Science and Engineering*, **143**, 3, 226–239 (2003).

3. A. K. PRINJA, "On the master equation approach to transport in discrete random media in the presence of scattering," *Annals of Nuclear Energy*, **31**, 2005–2016 (2004).

4. R. VASQUES, *A review of particle transport theory in a binary stochastic medium*, Master's thesis, Universidade Federal do Rio Grande do Sul (2005).

5. A. J. OLSON, A. K. PRINJA, and B. C. FRANKE, "Radiation transport in random media with large fluctuations," *Trans. Am. Nucl. Soc.*, p. 357.

6. R. VASQUES, R. N. SLAYBAUGH, and K. KRYCKI, "Nonclassical particle transport in the 1-D diffusive limit," *Trans. Am. Nucl. Soc.*, p. 361.

7. S. D. PAUTZ and B. C. FRANKE, "An atomic mix closure for stochastic media transport problems," *Trans. Am. Nucl.*
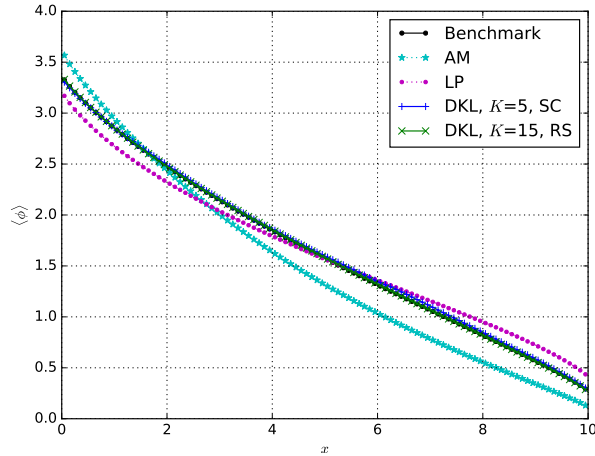
Fig. 6. Flux mean, Case 3a, *L*=10.0
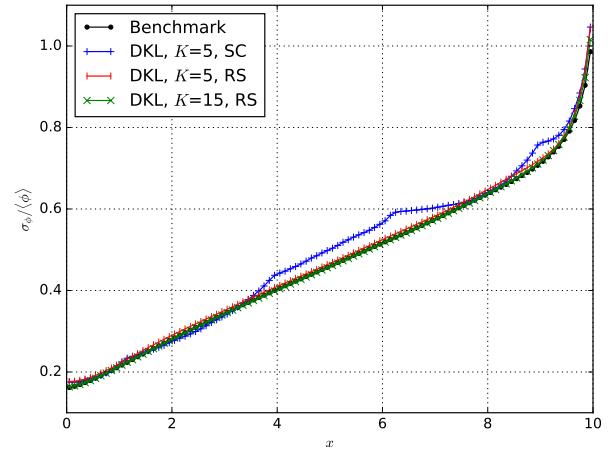
Fig. 7. Flux relative standard deviation, Case 3a, *L*=10.0
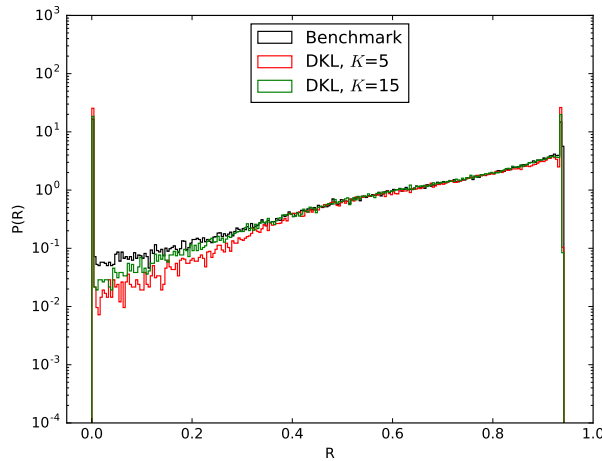
Fig. 8. Reflectance pdf, Case 3a, *L*=10.0
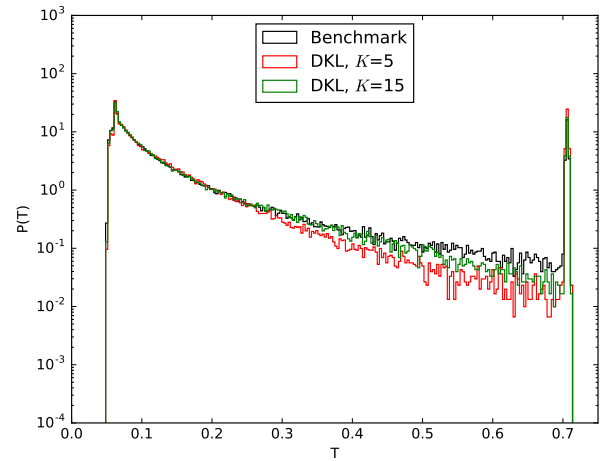
Fig. 9. Transmittance pdf, Case 3a, *L*=10.0

Soc., p. 365.

8. P. S. BRANTLEY, "Modified closures in Monte Carlo algorithms for diffusive binary stochastic media transport problems," *Trans. Am. Nucl. Soc.*, p. 369.

9. M. L. ADAMS, E. W. LARSEN, and G. C. POMRAN-ING, "Benchmark results for particle transport in a binary Markov statistical medium," *Journal of Quantitative Spectroscopy and Radiative Transfer*, **42**, 4, 253–266 (1989).

10. P. S. BRANTLEY, "A benchmark comparison of Monte Carlo particle transport algorithms for binary stochastic mixtures," *Journal of Quantitative Spectroscopy and Radiative Transfer*, **112**, 599–618 (2011).

11. G. B. ZIMMERMAN and M. L. ADAMS, "Algorithms for Monte-Carlo particle transport in binary statistical mixtures," *Trans. Am. Nucl. Soc.*, **63**, 287 (1991).

12. S. J. J. ILANGO, S. SARKAR, and A. SAMEEN, "Re-construction of 2-D porous media using Karhunen-Lóeve [sic] expansion," *Probabilistic Engineering Mechanics*, **32**, 56–65 (2013).

13. A. PARK, M. M. R. WILLIAMS, A. K. PRINJA, and M. D. EATON, "Modelling non-Gaussian uncertainties and the Karhunen-Loève expansion within the context of polynomial chaos," *Annals of Nuclear Energy*, **76**, 146–165 (2015).

14. F. NOBILE, R. TEMPONE, and C. G. WEBSTER, "An anisotropic sparse grid stochastic collocation method for partial differential equations with random input data," *SIAM Journal of Numerical Analysis*, **5**, *46*, 2411–2442 (2008).

15. B. M. ADAMS, M. S. EBEIDA, M. S. ELDRED, ET AL., "Dakota, a multilevel parallel object-oriented framework for design optimization, parameter estimation, uncertainty quantification, and sensitivity analysis: Version 6.5 theory manual," Tech. Rep. SAND2014-4253, Sandia National Laboratories (2016).

16. O. P. LEMAÎTRE and O. M. KNIO, *Spectral methods for uncertainty quantification: With applications to computational fluid dynamics*, Sprinter Dordrecht Heidelberg London New York USA, 1st ed. (2010).

17. T. GERSTNER and M. GRIEBEL, "Dimension-adaptive tensor-product quadrature," *Computing*, **71**, 65–87 (2003).

18. A. J. OLSON, *Reduced-order Monte Carlo modeling of*
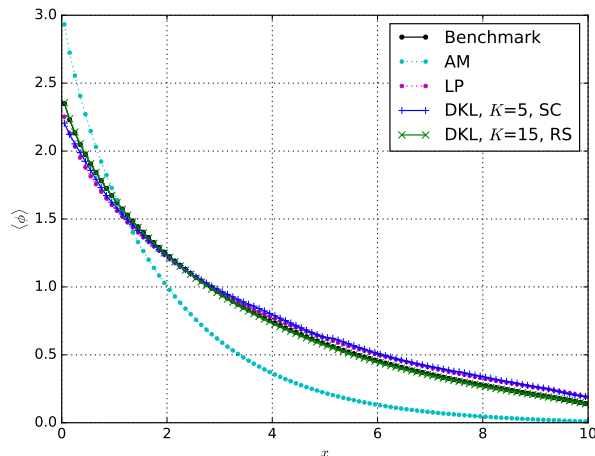
Fig. 10. Flux mean, Case 2a, *L*=10.0
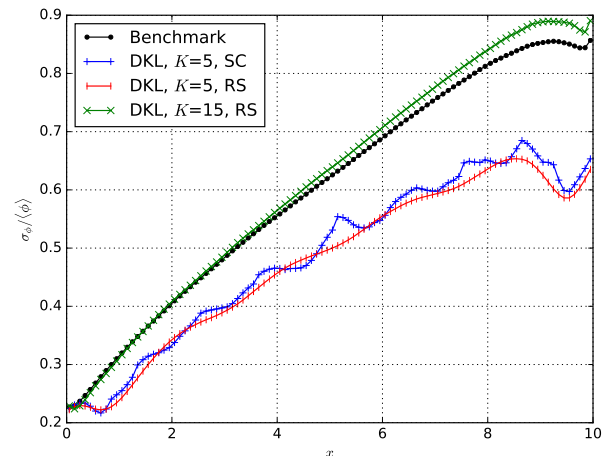
Fig. 11. Flux relative standard deviation, Case 2a, *L*=10.0
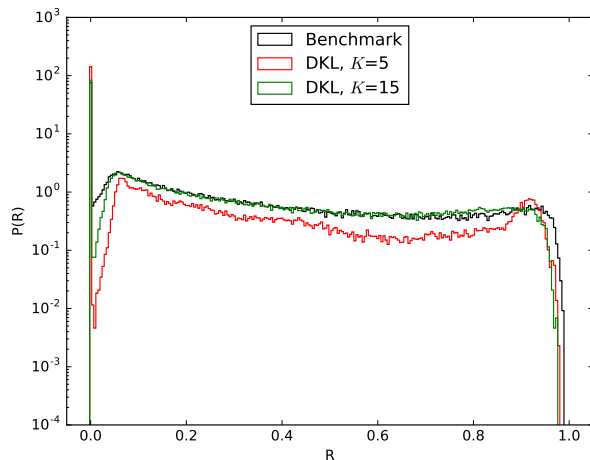
Fig. 12. Reflectance pdf, Case 2a, *L*=10.0
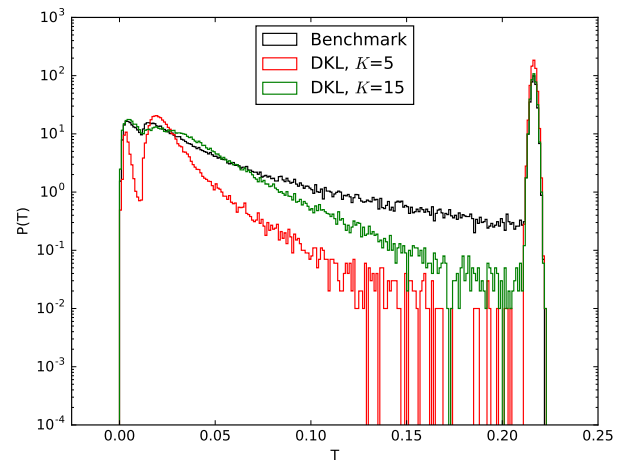
Fig. 13. Transmittance pdf, Case 2a, *L*=10.0

radiation transport in random media, Ph.D. thesis, University of New Mexico (2016).

19. J. W. FENG, C. F. LI, S. CEN, and D. R. J. OWEN, "Statistical reconstruction of two-phase random media," *Computers & Structures*, **137**, 78–92 (2014).

20. A. J. OLSON, A. K. PRINJA, and B. C. FRANKE, "Woodcock Monte Carlo transport through binary stochastic media," *Trans. Am. Nucl. Soc.*, **111**, 651 (2014).

21. E. D. FICHTL and A. K. PRINJA, "The stochastic collocation method for radiation transport in random media," *Journal of Quantitative Spectroscopy and Radiative Transfer*, **112**, 4, 646–659 (2011).

22. A. J. OLSON, A. K. PRINJA, and B. C. FRANKE, "Radiation transport in random media with large fluctuations," in "RPSD 2016," American Nuclear Society, Paris, France (October 2016).

23. E. JONES, T. OLIPHANT, P. PETERSON, ET AL., "SciPy: Open source scientific tools for Python," (2001–), [Online; accessed 2017-02-10].

24. W. BETZ, I. PAPAIOANNOU, and D. STRAUB, "Assessment of methods for the numerical solution of the

Fredholm integral eigenvalue problem," in "11th International Conference on Structural Safety & Risk 2013," International Association for Structural Safety & Reliability, New York, NY (June 2013).

25. S. SUN, J. ZHAO, and J. ZHU, "A review of Nyström methods for large-scale machine learning," *Information Fusion*, **26**, 36–48 (2015).

26. L. L. CARTER, E. D. CASHWELL, and W. M. TAYLOR, "Monte Carlo sampling with continuously varying cross sections along flight paths," *Nuclear Science and Engineering*, **48**, 403–411 (1972).